Odor- and context-dependent modulation of mitral cell activity in behaving rats

Leslie M. Kay and Gilles Laurent

Division of Biology, 139-74, California Institute of Technology, Pasadena, California 91125, USA
Correspondence should be addressed to G.L. (laurentg@cco.caltech.edu)

The projections and odor responses of mammalian olfactory receptor neurons, as well as the physiology of the bulb's principal neurons—the mitral cells (MCs)—are known from studies in slices and anesthetized animals. In behaving rats trained to discriminate between two odors associated with different reinforcers, we examined MC responses following alternated odor–reinforcer pairings. Whereas only 11% of the recorded MCs showed changes in odor-selective firing rate during the odor-sampling phase, 94% of MCs modulated activity during specific behaviors surrounding odor sampling. These cell- and odor-selective responses were not primary sensory responses; rather, they depended (reversibly) on the predictive value of each odor. MC activity thus depends critically on efferent influences linked to the animal's experience and behavior.

Studies of MC odor responses in anesthetized rats and rabbits show that MCs in defined regions of the OB respond to sets of similar odorant chemicals (for instance, volatile aliphatic alcohols), whereas distant ones respond to different compounds (for instance, aromatic compounds)[1–4]. Other studies, however, suggest that MCs responding to particular odorants can be found in all regions of the OB, and that most cells respond to many different odorants belonging to many physicochemical groups[3,5].

What is known about OB activity in awake, behaving animals? Field potential recordings from awake rabbits classically conditioned to odorants present a complex picture of OB activity during behavior. Although spatially coherent, local field potentials (LFPs) of the OB show spatial amplitude patterns that can be used to classify the odorants presented and their contingency[6]. These macroscopic patterns drift with time, abruptly changing when the meaning of the odor (that is, whether the reinforcer is positive or negative) is changed. This could be explained by context-dependent population dynamics, influenced by feedback from forebrain areas, of neuron assemblies underlying the LFP[7–11]. Here, we addressed this more directly.

Recordings from single mitral cells in awake or behaving mammals remain scarce[12–15]. Mitral cell activity (firing rate and respiratory patterning) is variably and inconsistently related to an odor and to the behavioral responses it evokes in these studies. Possible behavioral influences on MC sensory activity might be obscured by the complexity of experimental designs in these studies. Also, encoding of an odor by MC arrays *in vivo* may not be detectable or decipherable from firing rates of individual cells[16]. We addressed these issues by considering MC activity in behaving rats trained to discriminate two odors associated with different reinforcers. Our goal was to identify odor related or other features of the animal's environment and behavior that reliably influenced MC activity.

Results

Behavior and cell identification

Our protocol was based on odor-cued taste avoidance[17] (see Methods). Two odorants were used in each experiment, and each rat sequentially performed up to three different odor-association tasks in successive behavioral phases P1–P3 (**Fig. 1a** and **b**). In P1, the animal learned to associate each of two odorants with a reward of 10% sucrose. In P2, one of the two odors was paired with a quinine solution (aversive) and the other was paired with 30% sucrose. The animals learned this change in contingency (avoided drinking the solution associated with quinine on the basis of the CS–odor) within five to ten CS–trials (**Fig. 1a**). We assayed learning by the delay between odor onset (door opening) and drinking onset. In P3, each of the two odors was reverted to its P1 contingency (both odors paired with 10% sucrose). Animals very rapidly (in < 10 trials) reverted to their P1 behavioral patterns (chose either odor). These three behavioral phases were preceded by control trials in which either nothing happened (N, **Fig. 1a**) or the animal was given a 10% sucrose solution without associated odor (S, **Fig. 1a**).

Mitral cell activity was recorded using a tungsten-electrode array placed above the medial portion of the dorsal olfactory bulb (see Methods). Recordings were made from both dorsal and ventral mitral cell layers. In 23 sessions with 5 animals, we obtained 52 unambiguously discriminated individual cells (**Fig. 1b**) and 3 multiunit recordings. In 12 of these sessions, 2–5 cells were each recorded from different electrodes, and in 10 sessions, multiple (2–3) cells were recorded from a single electrode. The firing rates of the cells ranged from 1 to 33 Hz, with the majority below 20 Hz (mean, 12.1 ± 8.2 Hz; mode, 9 Hz; median, 9.5 Hz) and one unique cell at 54 Hz. Most of the cells were presumed mitral or tufted cells, based on their firing rates[12,14,15], depth of recording sites[18], electrophysiological characteristics of the surrounding areas (see below and **Fig. 2**), homogeneity of spike waveforms (**Fig. 1b**)

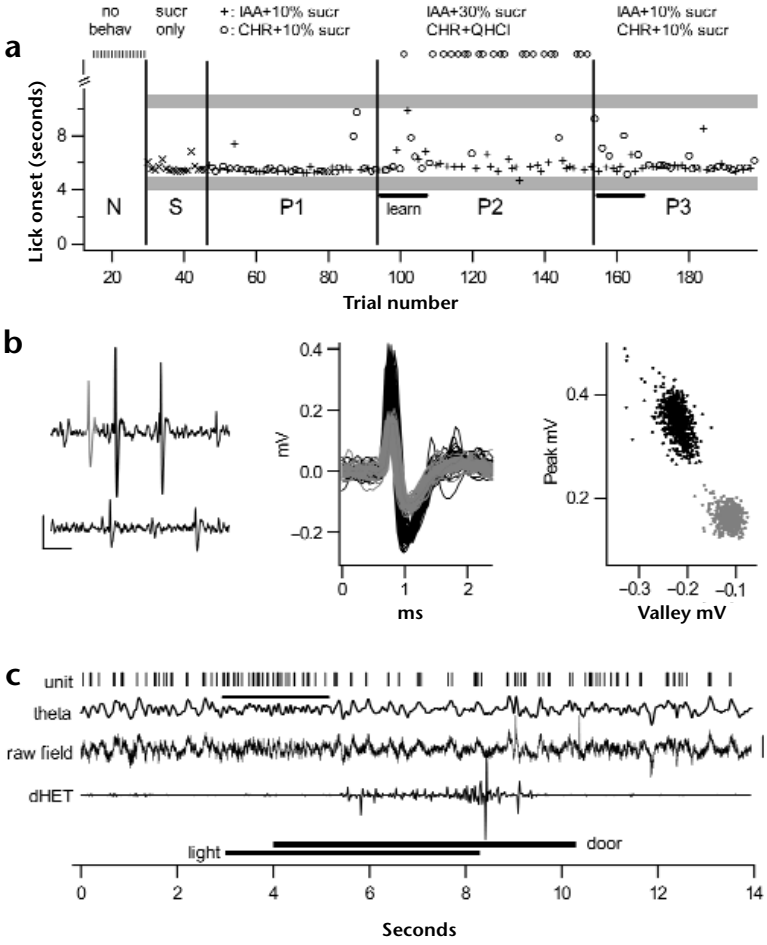

Fig. 1. Behavioral paradigm, mitral cell unit isolation and experimental design. (**a**) Each recording session contained up to 250 successive trials (*x*-axis) delivered at 20–60-s intervals. The session was divided into several phases (N, S, P1–3; see text). The *y*-axis represents time within each trial when drinking started. Horizontal gray bars indicate timing of door opening and closing. Markers signify the drinking onset time for each trial. Markers at the top represent trials in which the rat did not drink. N (|), no odors or behavior. S (×), 10% sucrose only. P1–P3: IAA (+), isoamyl acetate; CHR (○), cherry. P1: IAA and CHR, both in 10% sucrose. P2: CS+, IAA + 30% sucrose; CS–, CHR + QHCl. Note initial increase in drinking latency for both odors, followed, after approximately 10 trials, by 90% selective avoidance of CHR + QHCl. P3: same as P1. Note rapid return to behavior as in P1 (extinction of CHR avoidance). The average onset times of licking in S, P1, P2 (CS+ trials), and P3 are statistically indistinguishable. Learning trials are noted by the dark underbar in P2 and P3. (**b**, left) Sample data from two microelectrodes. The simultaneously recorded top and bottom traces show two and one well-defined waveforms, respectively. Scale bars, 200 μV, 5 ms. (**b**, middle) Spike waveforms from 2 cells extracted from data represented in left figure. (**b**, right) Cluster segregation of spike waveforms in middle panel. (**c**) Single 14-s trial showing a spike raster from a mitral cell (unit), the theta band of the field potential (3–15 Hz), the raw field potential from a microelectrode (1–250 Hz), the time derivative of the HET 'lickometer' signal (dHET) and the durations and timing of the light signal and door opening. A period of rapid sniffing beginning with the onset of the light stimulus is marked with a heavy bar over the theta signal. Most trials follow this pattern, providing some consistency in behavior. Scale bar (to right of raw field trace), 200 μV.

and post-mortem histological reconstruction of the electrode tracks (**Fig. 2**). Because each animal was used over many recording sessions, we could not lesion the recording site or kill the animal for histological confirmation after each session. We confirmed cell identity in 3 separate animals using silicon-electrode arrays[19] of 16 aligned recording pads (100 μm inter-pad interval; **Fig. 2**). Each electrode collected LFP and unit activity along one axis. The mitral cell layer and location was identified by physiological criteria and later confirmed histologically (**Fig. 2**); electrophysiological characteristics of the cell layers were similar to those recorded with tungsten electrodes (detectable unit activity in the mitral cell layer and internal plexiform layer, undetectable or low unit activity in the external plexiform or granule cell layer).

Half of the neurons (26 of 52) were at least weakly or intermittently modulated by respiration. Of these, seven were strongly modulated by respiration, and four of these seven maintained respiratory modulation during fast sniffing associated with odor identification. Of the 19 neurons that were weakly or intermit-

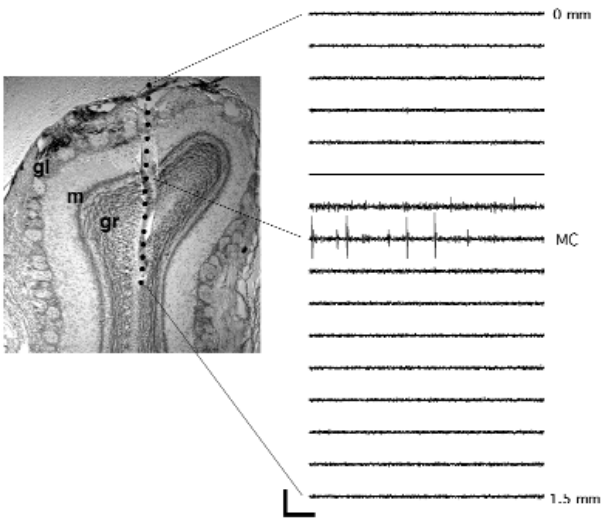

Fig. 2. Identification of recording sites in the OB using a 16-channel silicon probe. A 60-μm-thick section of the left medial dorsal OB (left), with electrode track and location of recording sites. Topmost recording site is at the dorsal surface, identified by lesions and serial sectioning. Recording sites were 100 μm apart and 177 μm^2 in surface area. High-frequency signals (600–9000 Hz; right) recorded from the probe indicated to left. The eighth recording site from the top shows prominent mitral cell spikes. The seventh and ninth sites show higher background activity (including small amplitude spikes) than the other sites. The flat line at channel 6 represents a defective lead on this probe. Scale bars, 200 μV and 20 ms.

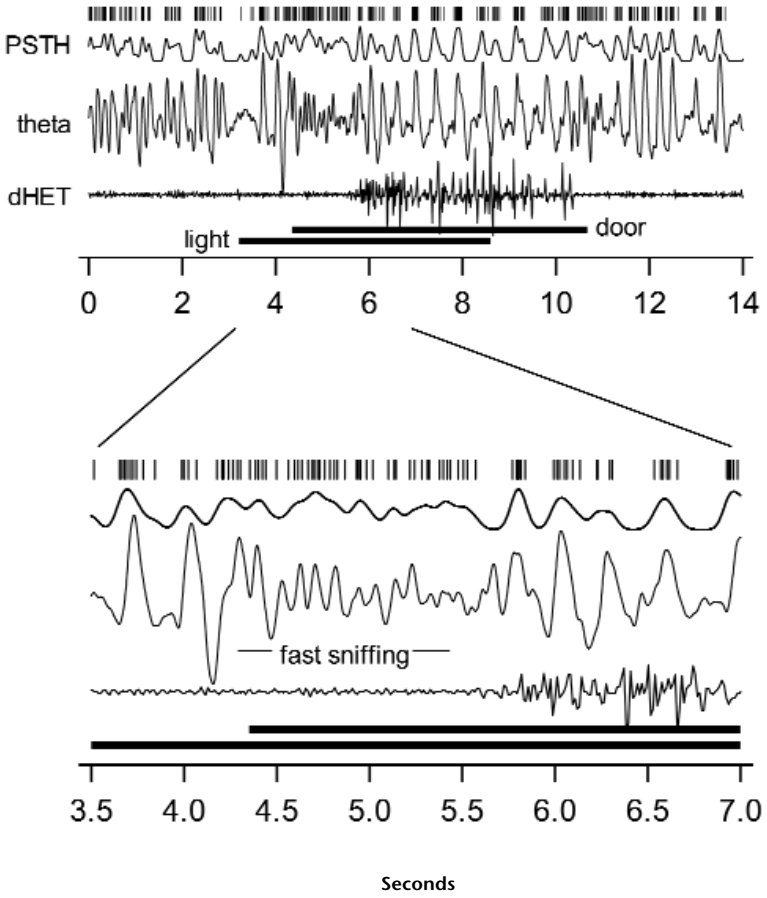

Fig. 3. Respiratory driving of single units. A 14-s trial showing a unit raster (top), smoothed peristimulus time histogram (PSTH), theta band LFP (theta), HET signal (dHET), and light and door markers. (bottom) Expanded 3.5-s segment centered on the fast-sniffing period associated with odor identification. The theta band signal followed the rat's respiratory cycle; upward deflections indicate inhalation[34,35]. This unit showed moderate respiratory driving during the prestimulus period of lower frequency (3–6 Hz) respiration. As the door opened at 4.4 s (when the odor became available), the rat sniffed at a higher rate (10 Hz), and respiratory patterning of the MC's activity was lost. The door was fully raised at 5.4 s, and drinking began at approximately 5.7 s. At this point the respiratory frequency dropped to ~2.5 Hz and patterning resumed as the animal began drinking.

tently modulated by respiration, only 2 maintained weak respiratory locking during the sniffing period. In all other cells, we confirmed interruption of respiratory patterning during rapid sniffing[14,15] (**Fig. 3**), which precluded analyzing coherence between unit and respiratory cycling. This differed from the strong synchronization of MCs with respiration seen in urethane-anesthetized animals[20].

Odor- and behavior-driven activity modulation

We examined MC activity during the 40–60 trials within each behavioral phase, S and P1–3 (**Fig. 1c**). Each 14-second trial consisted of several periods (wait, move to door, sniff, drink/not drink, withdraw). All trials in one phase were aligned on the light onset to build rasters of MC activity around the time of odor identification (**Fig. 4a**). Nearly all individual cells (49 of 52) and 3 of 3 multiunit recordings showed significant modulation of firing rate over one or more specific periods of the 14-second odorless control trials (S, **Fig. 4a**; $p < 0.05$). The cell shown, for example, showed significantly higher activity immediately following the light signal and as the door opened, and lower activity during drinking. The range and reliability of this activity can be compared to that recorded during random idle 14-second episodes (N; **Fig. 4a**).

We next considered effects of odors and odor–reinforcer contingencies. Firing patterns were both behavior- and cell-specific. Most cells retained similar modulation patterns as long as behavioral requirements and odor–reinforcer contingency remained constant. When these changed, the modulation pattern also changed (**Fig. 4b**, same neuron as in **Fig. 4a**). Each panel (**Fig. 4b**) represents the firing behavior of that neuron during one of the three behavioral phases with odors (P1–3, respectively). Each curve within each panel represents the neuron's firing pattern in one of the two odor–reinforcer contingencies (**Fig. 4b**). Differences in the histograms (P2) occurred when behavioral responses to the odors were different (drink versus no drink), as was the case for most modulated cells (44 of 49). Animals drank during very few CS– trials, and behavioral responses differed significantly between CS– lick and CS+ drink trials (delayed and short duration licks for CS–). We were therefore unable to associate differences in the CS+ and CS– histograms in P2 with motor differences.

We found that, first, the strongest predictor of changes in firing pattern was not the odor itself, but the reinforcer and behavior associated with that odor. For example, the firing profiles of the neuron in Fig. 4b in the presence of either odor were indistinguishable in P1 (both odors paired with sucrose; **Fig. 4b**), but significantly different when one odor was associated with quinine (P2, **Fig. 4b**; $p < 0.001$ for 94% and $p < 0.05$ for 6% of modulated cells). Second, if the contingencies were returned to the initial conditions, firing patterns also reverted (became indistinguishable again; P3, **Fig. 4b**), showing that these modulation patterns were stable over the course of an experiment. Third, we detected significant differences between firing patterns (as seen in **Fig. 4b**) in 44 of the 49 modulated cells and in 2 of 3 multiunit recordings only after the onset of drinking (well after the olfactory-discrimination phase). In 10 of the 49 modulated cells, this modulation was significant only for a subset of the odor–behavior contingency pairs. For example, a cell could show significant modulation in P1, but not in P2, or for both odors in P1 but only one odor in P2 (six cells). Fourth, we found that firing patterns and their behavior-related modulations were cell-specific. Cells recorded simultaneously on different electrodes (**Fig. 5**) showed different firing profiles. Conversely, cells recorded from the same electrode always had similar profiles. Fifth, only 5 of 52 individual cells and 1 multiunit recording showed odor-selective firing rate differences during odor identification (after door opening but before drinking). Figure 6 shows PSTHs for two simultaneously recorded individual cells with significant differences in odor-selective firing rate during the sniffing period. Whereas cell 1 showed this difference in phase P2 ($p < 0.05$), cell 2 showed it in P1 ($p < 0.01$). In both cells, odor-selective firing-rate differences changed with odor contingencies.

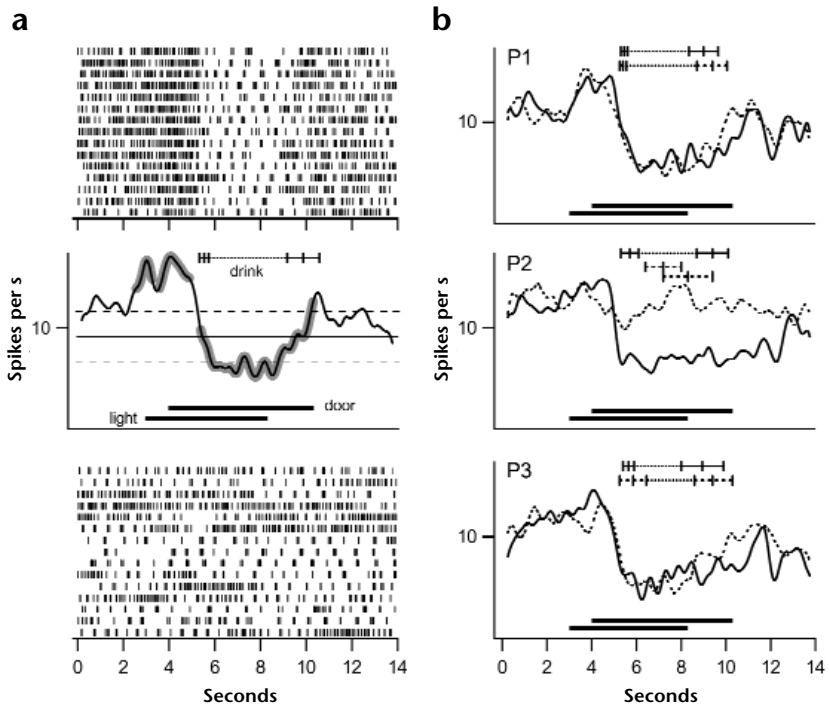

Fig. 4. Behavioral modulation of firing rate. (**a**) Control trials (phase S) showing behavior-related modulation in firing rate. Spike rasters (top) are given for one mitral cell on successive trials. Smoothed histogram (middle panel; 500-ms Gaussian convolved with the spike train, averaged across trials; first and last 250 ms omitted because of smoothing) constructed from rasters in top panel. Gray shaded portion of curve indicates periods in which the firing rate was significantly different from that in the first second of the trial. Plain and dashed horizontal lines indicate for comparison the mean ± s.d. of the firing rate in control trials with no stimulus or behavior (rasters in bottom panel). Line labeled 'drink' shows the mean ± s.d. of the start and end of drinking for sucrose control trials (n = 15). Light-on and door-open durations are marked below the curve. (**b**) Contingency-specific firing patterns. Data from cell in Fig. 4a showing behavior-related modulation of firing rate in response to odor stimulation and learning. Smoothed histograms are shown for two odor conditions (solid curve, odor A, isoamyl acetate/IAA; stippled curve, odor B, cherry) and three behavioral phases (P1–P3), as indicated on figure. Drink markers and trial markers as in Fig. 4a (odor A, top; odor B, bottom). P1, both odors in 10% sucrose solution (odor A, n = 20; odor B, n = 21). P2, odor A in 30% sucrose (n = 23); odor B in QHCl solution (n = 22), with the rat licking on only 2 trials (represented in the overlapping start and end drink markers). P3, post-extinction trials with both odors in 10% sucrose solution (odor A, n = 20; odor B, n = 20). Shape of histograms in P1 was the same as that in Fig. 4a, and there was no significant difference between the two odors. In P2, the histogram associated with IAA was unchanged from P1, whereas that associated with cherry was significantly different, but only after the time corresponding to the onset of drinking for IAA. The animal did not drink in most trials after sniffing cherry + QHCl solution (lick; n = 2). In those trials in which the rat licked, the onset of licking was significantly delayed relative to that for IAA trials. Post-extinction trials in P3 show return of firing profiles to those seen in P1. Learning trials at the beginning of P2 and P3 were not included in the analyses.

Discussion

Nearly all cells recorded in the OB during these naturalistic odor-cued and learning tasks showed significant modulation of firing rate that depended not only on the odor, but also on its contingency or predictive value. Odor-selective differences in firing rate were detected during the odor-identification period preceding a behavioral decision (drink or avoid) in only 11% of the cells. However, we observed significant modulation of firing rate during the odor-driven behavior in 94% of the cells. These context-selective modulation patterns—whether during or after the odor identification period—could be abruptly (within five to ten CS– trials) modified by a change in the odor–reinforcer contingency, and re-established by returning to the original contingency. This shows that responses, measured as significant modulations of firing rate, of OB neurons (first order olfactory neurons, located one synapse away from the receptors) were strongly influenced by efferent 'contextual' input, consistent with macroscopic field-potential studies[21,22]. Electrode depth, electrophysiological characteristics of the recording site, firing rate and histology all indicate that the majority of cells were probably mitral or tufted cells.

Could the animal's decision to drink or avoid be due to olfactory detection of the reinforcer (sucrose or quinine), rather than the intended odorant? Several results argue against this. First, the ability of a rat to discriminate sucrose concentrations can be masked by another odorant[23]. Second, the concentration of QHCl that we used is one-tenth of the lowest concentration at which

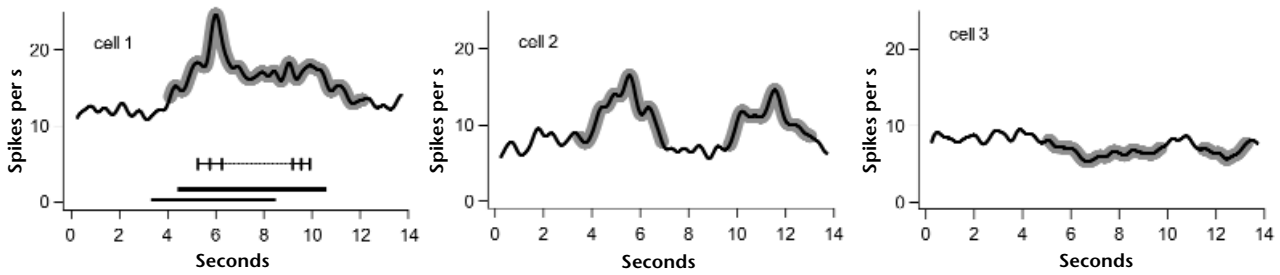

Fig. 5. Behavior-associated modulations in firing rate for three cells recorded simultaneously from three different electrodes. Histograms and markers generated as in Fig. 4 (n = 18). Each cell had its own characteristic modulation pattern, demonstrating that the modulation is not necessarily linked to increases or decreases in sniffing rate. Background firing rates, 6–12 Hz. Shaded portions of curves as in Fig. 4a.

rats in a previous study[17] could detect QHCl in plain dH_2O and below the level of detection in dH_2O for most similar salts[24]. Third, in randomized trials using the same odorant in either sucrose or quinine solution, the animal performed at chance level (17 of 29 trials correct; $p > 0.3$), indicating its inability to discriminate between the two solutions on the basis of the odor of the US. These behavioral results do not rule out the possibility that an individual cell can respond to either sucrose or quinine. However, the sucrose trials at the beginning of an experiment produced a histogram similar to that from the odor trials in phase P1 (**Fig. 4**). Similarly, during training in P2, the histogram for trials during which the animal drank for an extended period in response to CS– (2–7 trials) was of similar shape to that for CS+ trials from P1 or P2. This suggests that the slow temporal patterns were a product of context and behavior, rather than the odor of sucrose or quinine.

Our failure to detect odor-selective responses in nearly 90% of the cells does not mean that they were not involved in odor encoding. Rather, this result probably has at least two explanations. First, although most of the odors used were complex mixtures or odors known to activate large portions of the OB[25,26], our stimulus set may have been too small to elicit any response in the majority of recorded cells. Second, slow modulations of firing rate may not be the best measure of a cell's involvement in odor representation or coding. If, for example, odors are represented by dynamical and relational aspects of firing within large assemblies of neurons, short increases and decreases in firing rate of an individual cell may easily pass undetected. Detection of such events is made all the more difficult by the complex and variable nature of odor sampling by behaving animals. Hence, averaging of responses for multiple trials aligned on stimulus onset may smear out fine features of the response. This analysis, therefore, could only reliably detect slow features in MC responses and their relation to odor-driven behavior. It is these results that seem important to us, precisely because they reveal reliable effects of 'prior knowledge' and behavior on MC activity.

Our results show that MC output was strongly and dynamically influenced by recent experience with an odor. MC firing rate was reliably modulated during specific phases of olfactory behavior, especially at times other than that of actual odor discrimination. This behavioral modulation was odor dependent in an associative rather than in a primary sensory sense. It was reliable under constant testing conditions with rigorously controlled behavior. These results extend and possibly explain previous similar observations obtained with LFP recordings[6]. They suggest, therefore, that MCs may be under strong control by efferent 'contextual' output from olfactory cortex and associated areas[22]. Neurons in orbitofrontal cortex and the amygdala fire in a context-dependent fashion during an olfactory discrimination task similar to that used here[27,28]. Strong bidirectional anatomical connections between the amygdala, olfactory cortex, orbitofrontal cortex, hippocampus and olfactory bulb exist in all mammals studied[7–11] and may contribute to the effects observed here. We found that behavioral modulation of MC firing was cell-specific, but that MCs recorded with the same electrode underwent similar influences, whereas MCs with different modulation profiles were always recorded from different electrodes. This suggests that efferent influences may be somewhat local.

Our results extend the few previous studies of MC odor responses in awake or behaving mammals[12–15], which include analyses of firing rate, phase of the respiratory cycle during which a cell fires, respiration frequency[12–15] and correlation of single unit activity to contralateral multiunit activity[12], both for patterns and variability. Patterning of responses is most reliable during slow breathing, in the odorless phases of those experiments, or after the first part of the odor stimulus, when the animal's breathing rate slows[12–15]. In anesthetized rodents, the phase of firing relative to the respiratory cycle during slow breathing

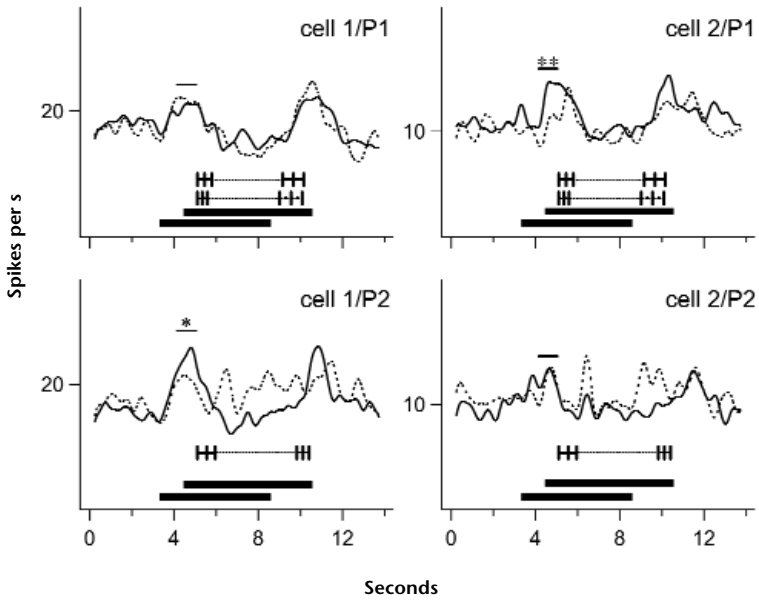

Fig. 6. Odor-selective differences in firing rate during odor identification. Histograms were smoothed as in Figs. 4 and 5. Results for two simultaneously recorded cells are shown (cell 1, left column; cell 2, right column) for the two behavioral phases completed in this experiment (P1, top row; P2, bottom row, as described in **Figs. 1a** and **4**). Solid curves represent the histograms from odor A (apple) trials, and stippled curves, histograms from odor B (strawberry) trials, as described in Fig. 4 legend. Door (top) and light (bottom) markers are shown below each set of histograms. Drinking start and end times (± s.d.) are also shown for each odor class in P1 (upper, odor A, $n = 19$; lower, odor B, $n = 16$ and for odor A (CS+) in P2 (animal did not drink during the CS– trials in P2; odor A or B, $n = 16$). The time between the beginning of the door opening to the beginning of drinking is considered the odor-identification period. Horizontal lines above the traces in each figure indicate the test period for odor discrimination (1.0 s; $^*p < 0.05$, $^{**}p < 0.01$). Significant differences in firing rate were found between odors in the two cell/behavioral phase combinations, indicated with asterisks. In the remaining two figures, no significant differences were found. By this measure, cell 1 gained odor-selectivity with learning in P2, whereas cell 2 lost odor selectivity from P1 to P2. Baseline firing rates were unchanged between P1 and P2. For all six cells showing odor selectivity, these differences remained significant over a range of window sizes during the odor-identification period. Three of the individual cells and the multiunit recording showed significance ($p < 0.01$) during the original one-second window. The remaining 2 cells had values of $p < 0.05$ using a 1-s window, or $p < 0.01$ using a 0.8-s window for one cell and a 1.2-s window for the other cell. The differences for the two odorants during the sniffing period were independent of differences in sniffing rate, as rates did not significantly differ across odorants.

(0.7–4 Hz) is predictive of odor quality[29]. Respiratory patterning significantly decreases and variability of firing patterns and responses increases when respiratory rate increases to 5–10 Hz[12–15]. Such fast sniffing corresponds to that associated with odor identification in our study. The relatively stable relationships between respiratory cycle and odor responses seen previously seem to occur during slow breathing associated with odor habituation or anesthesia[30,31], rather than during odor identification. Thus, this measure may not be reliable in a directed behavioral task involving rapid sniffing and odor identification.

Our study shows a picture of MC activity different from that seen in studies exploring spatial odor mapping in the OB of anesthetized mammals[1–5]. Although different groups find partly contradictory results[2–5], odor responses are described as stable. We found that, in the few neurons that showed odor selectivity, these responses changed when the meaning of the odorant changed. Thus, as in other systems, MC activity may represent different functions in behaving, passively awake or anesthetized animals, as seen in other systems[32,33]. These differences are probably driven by the vast network of efferent and neuromodulatory inputs to the OB, many of which could be altered with anesthesia or may depend on behavioral state. They could also be caused by motor, sensory (odor or taste) or emotional changes over the course of the odor-guided behavior.

In conclusion, our study indicates that MC firing rates in behaving rats can be consistent and reliable, provided that the animal's behavior is heavily constrained by externally imposed markers (for example, light signals, door openings, odor onset and offset). We find that signals carried by MCs from the OB to the rest of the CNS may already, at this peripheral stage, be strongly influenced by efferent, contextual inputs and likely contain a significant amount of non-primary sensory information.

Methods

Behavior. Five adult male Sprague-Dawley rats (3–6 months; Simonsen Labs) were trained to a simple behavioral task with no odorant stimulation before surgical implantation of electrodes. Over a three-to-five-day period they were familiarized with the test chamber and the timing of cues: at a random time, a light was turned on in the cage, indicating the opening of a door one second later and access to a drinking port. The rat could then drink sugar water (~0.05 ml) for 4 s, after which the light was turned off and the door closed one second later. Licking/drinking was detected using a Hall effect transducer (HET) placed next to the drinking tube, to which a small magnet was attached (**Fig. 1c**). A deviation from the flat baseline derivative of the HET signal (dHET) was seen only when the tube was deflected, as during licking. The relative timing of stimuli presented to each animal was kept constant (light on, door opening and closing, light off), while the length of control periods before and after each trial varied. We recorded activity for 10–14 s of each trial, centered on the light on/door closed period (**Fig. 1c**). The door took one second to open or close. Some rats retreated from the drinking port when the light was extinguished; others drank until the door closed.

Five to seven days after recovery from surgery, the animals were conditioned to the task and recordings were made with or without odors. Individual odorants were mixed into the sucrose or quinine solutions and were kept in separate syringes. As reported earlier[17], mixing the odorants in the solutions facilitated learning. We used three artificial blends (cherry, strawberry, apple from Aldrich and LorAnn Gourmet), one monomolecular odor (isoamyl acetate from Sigma), and two essential oils (vanilla, spearmint), none of which were aversive in solution to the animals. Concentration of all odorants was 0.01–0.05% (volume/volume). Positive air pressure was maintained inside the recording chamber so that an animal could smell the odor only when poking its nose into the small chamber behind the guillotine door. Thus, we could define the period in which the animal smelled and identified an odor as that period after the beginning of the door opening and before the onset of the CR (lick or no lick). In the cases when the correct response was no licking (CS– trials), the identification was presumed to have been made in the same length of time as in the CS+ trials. The respiratory rate was indistinguishable between the two types of trials in the one second after the door began to open.

Each recording session contained up to five phases (N, S, P1, P2, P3; **Fig. 1a**). There were no delays between phases other than the standard delay between trials (20–60 s). In phase N, 10–20 recordings were made as the rat rested. Phase S consisted of 10–20 odorless trials with plain 10% sucrose solution. In P1, each of two odors (A and B) was paired with the 10% sucrose solution (random order, balanced) in 40–60 trials. In P2, odor A (CS+) was paired with 30% sucrose and odor B (CS–) with quinine (0.0167%, weight/volume, or 5×10^{-4} M in distilled water; random order, balanced) in 50–70 trials. The rats learned within five to ten CS– trials to drink if they smelled A and to avoid or delay drinking if they smelled B. For two animals, CS+ was odor A in 10% sucrose and CS– was odor B in 10% sucrose plus quinine, which slowed learning. In most cases, odor discrimination was performed within 1.0–1.5 s after the opening of the door, evidenced by a fast drinking onset (**Fig. 1a**). Interestingly, a rat would occasionally taste the liquid associated with odor B (that predicting quinine; +, P2, **Fig. 1a**). In P3, the stimuli were returned to the P1 conditions, and the discriminative behavior was extinguished within a few trials (rat again drank for both odorant solutions with the same latency and duration).

In one experiment, we tested the ability of the rat to smell the difference between the CS+ and CS– solutions when they contained the same odorant. This was done after the P3 extinction trials (P4). Response time and its variance greatly increased and the animal performed at a level indistinguishable from chance ($p > 0.3$), although 'no drink' responses accompanied more CS– than CS+ trials (17 of 29 correct). Correct trials were assessed as for normal behavioral trials (P1–P3). Response times within two standard deviations of the mean response time for CS+ in P2 were 'drink' trials. Those with late or no response were 'no drink' trials. In P4, CS+ 'drink' trials were correct (7 of 15), and CS– 'no drink' trials were correct (10 of 14).

Electrophysiology. Each animal was implanted with 2–6 moveable microdrive probes in a circular array 1.5 mm in diameter (etched tungsten with 1-μm exposed tips, 2–5 MΩ impedance at 1 kHz) in one OB, and two 50-μm stainless steel wires at two different depths to record macroscopic field potentials at the surface and in the center of the same OB posterior to the microelectrodes. Each day the electrodes were moved individually in increments of 40 μm until cells could be located (**Fig. 1b**). The signals were then observed for 15–20 minutes to determine stability before recording. At the end of each session, the electrodes were backed out 40–160 μm to minimize damage to the mitral cell layer.

Neural data were recorded differentially using either of two reference leads, a skull screw or one of the non-optimally placed fine tungsten probes. Spike waveforms (2.75 ms) were extracted from signals sampled at 20 kHz (filters set at 0.6–9 kHz). Field potential signals from both the 1 and 50 μm probes were sampled at 0.5–1 kHz (filtered at 1–250 or 1–325 Hz). Data were recorded and behavioral signals controlled using Datawave Experimenter's Workbench 32, with Neuralynx Lynx-8 amplifiers and MedAssociates operant behavior modules. The recording cable contained a 17-channel JFET headstage with unity gain (NB Labs, Denison, Texas). Recordings for Fig. 2 were made using a silicon probe from the University of Michigan Center for Neural Communication Technology (16 channels with 100 μm recording pad separation[19]). The animal was anesthetized for this recording with a ketamine cocktail (ketamine/xylazine/acepromazine), which slightly increased activity in the olfactory bulb.

One to five cells were recorded during each session (two to three hours) on one to four electrodes. Most probes maintained a good signal-to-noise ratio (S/N > 3, up to 15) for several weeks. Recordings from most electrodes were isolated single units. When multiple single units appeared likely, their spike waveforms were separated using peak and trough amplitude and time, spike width, and other parameters. Interspike interval histograms were made to establish the presence of a refractory period of one to ten ms. When cells could no longer be isolated from the dorsal or

ventral mitral cell layer, the animal was perfused intracardially with buffered 10% formalin solution. The OBs were sectioned at 50 μm and stained with neutral red. Careful records were kept of electrode depths and movements, and the recording sites were estimated along with histological verification of electrode tracks. In two animals, electrolytic lesions were made in the final recording sessions. All cells were recorded either from the mitral cell layer (dorsal and ventral) or from the internal and external plexiform layers, close to the mitral cell layer.

All procedures involving animals conformed to protocols approved by the California Institute of Technology Animal Care and Use Committee with veterinary supervision by the Office of Laboratory Animal Research.

Analytical methods. All 10–14-s trials obtained with one odor, within one behavioral phase and with the same contingency were pooled to build rasters from each recorded MC (**Fig. 4**). All such trials were aligned at the onset of the light signal and used to build a smoothed peristimulus time histogram (PSTH) indicative of activity of each MC around and during olfactory behavior (**Fig. 4a**). Spike activity during seconds 2–14 of the trial was compared to that during the first second of the trial (when the animal was unaware of the impending trial).

Because olfactory behavior is nonstationary, we used relatively large bins to average the spike rate across trials in a behaviorally relevant fashion. Analysis of firing rate was performed on nonoverlapping 1-s windows across the set of trials for each phase of the experiment (P1–P3) and each odor-contingency class within each behavioral phase (odors A and B). The starting time of the binning was chosen so that the beginning of one bin corresponded with the beginning of the door opening. Firing rates were deemed to be significantly modulated at $p < 0.05$ in a one-way ANOVA across the 9–13 adjacent windows for each cell. Individual windows were then compared to the first one second of the trial (before the animals were aware that a trial had started) in a post-hoc test for significant deviation from this background firing rate ($p < 0.05$; Fisher's PLSD). Odor selectivity was determined by analysis solely of the bin preceding the onset of drinking (in the 1–1.5 s between door opening and onset of licking). A two-tailed *t*-test was performed for each cell on that bin across the two odor classes for each behavioral phase. We estimated sniffing rates (4–12 Hz) from the OB theta band LFP[34,35].

Acknowledgements

We are grateful to Steven Notari, Vali Mohammadi, Lindsey Drake and Maryellen Begley for assistance with surgery, electronics, histology and animal handling, to Lucia Jacobs for the loan of behavioral equipment (NSF grant IBN-9307317), to Mark Stopfer and Brian Smith for statistical advice, to Christophe Pouzat for assistance with the silicon probe recordings and to Erin Schuman, Rainer Friedrich and Mark Stopfer for comments on the manuscript. Silicon probes were obtained from the University of Michigan Center for Neural Communication Technology (NIH/NCRR grant P41-RR09754). Supported by grants from the Sloan Center for Theoretical Neuroscience at Caltech, the Keck Foundation, the Burroughs-Wellcome Center for Computational Molecular Biology at Caltech, the NSF and the NIDCD.

RECEIVED 15 JULY; ACCEPTED 2 SEPTEMBER 1999

1. Buonviso, N. & Chaput, M. A. Response similarity to odors in olfactory bulb output cells presumed to be connected to the same glomerulus: electrophysiological study using simultaneous single-unit recordings. *J. Neurophysiol.* **63**, 447–454 (1990).
2. Imamura, K., Mataga, N. & Mori, K. Coding of odor molecules by mitral/tufted cells in rabbit olfactory bulb. I. Aliphatic compounds. *J. Neurophysiol.* **68**, 1986–2002 (1992).
3. Mori, K., Mataga, N. & Imamura, K. Differential specificities of single mitral cells in rabbit olfactory bulb for a homologous series of fatty acid odor molecules. *J. Neurophysiol.* **67**, 786–789 (1992).
4. Katoh, K., Koshimoto, H., Tani, A. & Mori, K. Coding of odor molecules by mitral/tufted cells in rabbit olfactory bulb. II. Aromatic compounds. *J. Neurophysiol.* **70**, 2161–2175 (1993).
5. Motokizawa, F. Odor representation and discrimination in mitral tufted cells of the rat olfactory bulb. *Exp. Brain Res.* **112**, 24–34 (1996).
6. Viana di Prisco, G. & Freeman, W. J. Odor-related bulbar EEG spatial pattern analysis during appetitive conditioning in rabbits. *Behav. Neurosci.* **99**, 964–978 (1985).
7. de Olmos, J., Hardy, H. & Heimer, L. The afferent connections of the main and the accessory olfactory bulb formations in the rat: an experimental HRP-study. *J. Comp. Neurol.* **181**, 213–244 (1978).
8. Shipley, M. T. & Adamek, G. D. The connections of the mouse olfactory bulb: a study using orthograde and retrograde transport of wheat germ agglutinin conjugated to horseradish peroxidase. *Brain Res. Bull.* **12**, 669–688 (1984).
9. van Groen, T. & Wyss, J. M. Extrinsic projections from area CA1 of the rat hippocampus: olfactory, cortical, subcortical, and bilateral hippocampal formation projections. *J. Comp. Neurol.* **302**, 515–-528 (1990).
10. Carmichael, S. T., Clugnet, M. C. & Price, J. L. Central olfactory connections in the macaque monkey. *J. Comp. Neurol.* **346**, 403–434 (1994).
11. Jansen, H. T., Iwamoto, G. A. & Jackson, G. L. Central connections of the ovine olfactory bulb formation identified using wheat germ agglutinin-conjugated horseradish peroxidase. *Brain Res. Bull.* **45**, 27–39 (1998).
12. Pager, J. Unit responses changing with behavioral outcome in the olfactory bulb of unrestrained rats. *Brain Res.* **289**, 87–98 (1983).
13. Chaput, M. A. & Holley, A. Responses of olfactory bulb neurons to repeated odor stimulations in awake freely-breathing rabbits. *Physiol. Behav.* **34**, 249–258 (1985).
14. Pager, J. Respiration and olfactory bulb unit activity in the unrestrained rat: statements and reappraisals. *Behav. Brain Res.* **16**, 81–94 (1985).
15. Bhalla, U. S. & Bower, J. M. Multiday recordings from olfactory bulb neurons in awake freely moving rats: spatially and temporally organized variability in odorant response properties. *J. Comput. Neurosci.* **4**, 221–256 (1997).
16. Wehr, M. & Laurent, G. Odour encoding by temporal sequences of firing in oscillating neural assemblies. *Nature* **384**, 162–166 (1996).
17. Darling, F. M. & Slotnick, B. M. Odor-cued taste avoidance: a simple and efficient method for assessing olfactory detection, discrimination and memory in the rat. *Physiol. Behav.* **55**, 817–822 (1994).
18. Paxinos, G. & Watson, C. *The Rat Brain in Stereotaxic Coordinates* (Academic, New York, 1986).
19. Bragin, A. *et al.* Gamma (40–100 Hz) oscillation in the hippocampus of the behaving rat. *J. Neurosci.* **15**, 47–60 (1995).
20. Sobel, E. C. & Tank, D. W. Timing of odor stimulation does not alter patterning of olfactory bulb unit activity in freely breathing rats. *J. Neurophys.* **69**, 1331–1337 (1993).
21. Gray, C. M. & Skinner, J. E. Centrifugal regulation of neuronal activity in the olfactory bulb of the waking rabbit as revealed by reversible cryogenic blockade. *Exp. Brain Res.* **69**, 378–386 (1988).
22. Kay, L. M. & Freeman, W. J. Bidirectional processing in the olfactory-limbic axis during olfactory behavior. *Behav. Neurosci.* **112**, 541–553 (1998).
23. Rhinehart-Doty, J. A., Schumm, J., Smith, J. C. & Smith, G. P. A non-taste cue of sucrose in short-term taste tests in rats. *Chem. Senses* **19**, 425–431 (1994).
24. Miller, S. D. & Erickson, R. P. The odor of taste solutions. *Physiol. Behav.* **1**, 145–146 (1966).
25. Stewart, W. B., Kauer, J. S. & Shepherd, G. M. Functional organization of rat olfactory bulb analysed by the 2- deoxyglucose method. *J. Comp. Neurol.* **185**, 715–734 (1979).
26. Johnson, B. A., Woo, C. C. & Leon, M. Spatial coding of odorant features in the glomerular layer of the rat olfactory bulb. *J. Comp. Neurol.* **393**, 457–471 (1998).
27. Schoenbaum, G., Chiba, A. A. & Gallagher, M. Orbitofrontal cortex and basolateral amygdala encode expected outcomes during learning. *Nat. Neurosci.* **1**, 155–159 (1998).
28. Schoenbaum, G., Chiba, A. A. & Gallagher, M. Neural encoding in orbitofrontal cortex and basolateral amygdala during olfactory discrimination learning. *J. Neurosci.* **19**, 1876–1884 (1999).
29. Macrides, F. & Chorover, S. L. Olfactory bulb units: activity correlated with inhalation cycles and odor quality. *Science* **175**, 84–87 (1972).
30. Freeman, W. J., Viana Di Prisco, G., Davis, G. W. & Whitney, T. M. Conditioning of relative frequency of sniffing by rabbits to odors. *J. Comp. Psychol.* **97**, 12–23 (1983).
31. Gray, C. M. & Skinner, J. E. Field potential response changes in the rabbit olfactory bulb accompany behavioral habituation during the repeated presentation of unreinforced odors. *Exp. Brain Res.* **73**, 189–197 (1988).
32. Dave, A. S., Yu, A. C. & Margoliash, D. Behavioral state modulation of auditory activity in a vocal motor system. *Science* **282**, 2250–2254 (1998).
33. Schmidt, M. F. & Konishi, M. Gating of auditory responses in the vocal control system of awake songbirds. *Nat. Neurosci.* **1**, 513–518 (1998).
34. Klingberg, F. & Pickenhain, L. Über langsame atemsynchrone Potentiale vom Bulbus olfactorius der Ratte. *Acta Biol. Med. Ger.* **14**, 593–595 (1965).
35. Kay, L. M., Lancaster, L. R. & Freeman, W. J. Reafference and attractors in the olfactory system during odor recognition. *Int. J. Neural Syst.* **7**, 489–495 (1996).